Anchoring and orientational wetting of nematic liquid crystals on self-assembled monolayer substrates: An evanescent wave ellipsometric study

B. Alkhairalla, H. Allinson, N. Boden, S. D. Evans, and J. R. Henderson
Centre for Self-Organising Molecular Systems, University of Leeds, Leeds LS2 9JT, United Kingdom
(Received 8 September 1998)

An evanescent wave ellipsometric technique is used to study the orientational wetting of 4′,4-alkylcyanobiphenyls (nCB,$n=5$–9) at the interface with a series of self-assembled monolayers. Brewster angle measurements are interpreted in terms of a global orientational wetting phase diagram (T,n,h_1), where T denotes temperature, n is the alkyl chain length, and h_1 is the cosine of the contact angle of water with the monolayer. At temperatures below the isotropic-nematic phase transition temperature T_{IN}, an anchoring transition from planar to homeotropic alignment occurs as the surface of the monolayer is made more hydrophobic. Homeotropic anchoring of the nematic director at $T<T_{IN}$ is associated with complete orientational wetting on approaching the isotropic-nematic phase boundary from temperatures above T_{IN}. The anchoring-wetting transition shifts to less hydrophobic surfaces as n increases. [S1063-651X(99)12002-6]

PACS number(s): 61.30.−v, 64.70.Md, 68.45.Gd

I. INTRODUCTION

In the absence of external fields, the director of a nematic fluid N has no preferred orientation and thus fluctuates throughout space [1]. Surface treatments have been developed which pin the director parallel (planar anchoring) or perpendicular (homeotropic anchoring) to the surface. Anchoring is a mesoscopic phenomena, with the surface typically influencing the director orientation for some tens of μm into the nematic fluid. Traditionally, surface anchoring is induced by a variety of surface coatings and by rubbing to induce directional anisotropy in the case of planar alignment. However, the relationship between mesoscopic alignment and microscopic interactions is poorly understood. Statistical mechanics treats anchoring as a class of wetting phenomena [2,3]. Interactions that lead to complete wetting by nematic fluid at the substrate-isotropic interface might well be expected to induce a specific anchoring of the nematic director. The important order parameter associated with this class of wetting is not the density of the adsorbed film, but rather the orientation of the adsorbed molecules: so-called orientational wetting. Discontinuous jumps in the amount of adsorbed phase are also possible, known as first-order prewetting transitions [2,3].

Phenomenological theories of anchoring relate the quasi-macroscopic alignment to the free energy cost per unit area of bending the director, but little is known about the microscopic mechanisms involved [4–6]. In this paper we experimentally investigate the control of anchoring phenomena by variation of the intermolecular forces arising from a single monolayer. In addition, we explore the correlation between anchoring and orientational wetting. From theory, these phenomena lie in a three-dimensional phase space composed of temperature T and a second bulk thermodynamic field such as molecular shape n, which in our experiments define a surface of bulk isotropic-nematic phase transitions, together with a substrate field h_1. Variation of molecular geometry (such as molecular length) is possible using a homologous series of liquid crystal molecules. Shen and co-workers [7,8] used a series of 4′,4-alkylcyanobiphenyls (nCB's, where n is the number of carbon atoms in the alkyl chain) to traverse an orientational wetting transition on a single surface. Evans *et al.* [9] have explored orientational phase behavior as a function of the surface field h_1, for two values of n (5CB and 8CB). We now report a more wide ranging study, for the series of nCB's from $n=5$ to 9, on the same set of self-assembled monolayer (SAM) substrates. The surface field h_1 was controlled as in Ref. [9], by varying the ω-functional group of the long-chain alkylthiol SAM's [10–13]. The importance of these monolayer substrates lies in the ability to control the chemical composition of the outer surface of the monolayer, in a well-defined and robust manner. Here we use standard alkylthiols, $HS(CH_2)_mX$, chemisorbed onto gold films, varying the surface functional group X from hydrophilic ($X=$COOH,OH) to hydrophobic ($X=CH_3$). The thiol $HS(CH_2)_4OC_6H_4SCH_2(CF_2)_9CF_3$, [14] was used to generate a fluorinated hydrophobic surface. In all cases the aliphatic chains were long enough to form ordered crystalline monolayers.

To measure the orientational order in the interfacial region we have developed a Brewster-angle evanescent-wave ellipsometric technique [9]. Ellipsometric techniques have become an established research method for studying wetting phenomena at solid-fluid interfaces [8,15,16]. In our experiments the interfacial orientational order parameter that we measure is an integrated orientational adsorption lying within the range of an evanescent field generated at the substrate-fluid interface. Since the evanescent field decays exponentially into the liquid crystal phase (penetration depth $\sim$50 nm for our systems), this technique is more sensitive to changes occurring near the surface, as opposed to fluctuations in the bulk, and is therefore especially useful for investigating wetting phenomena. Moreover, since the light does not traverse the fluid sample, we can study wetting by opaque and birefringent fluids. The specific order parameter that we measure is the position of the Brewster angle, defined as being the angle with respect to the surface normal at which the real part of the ellipticity is zero [17]. Numerical

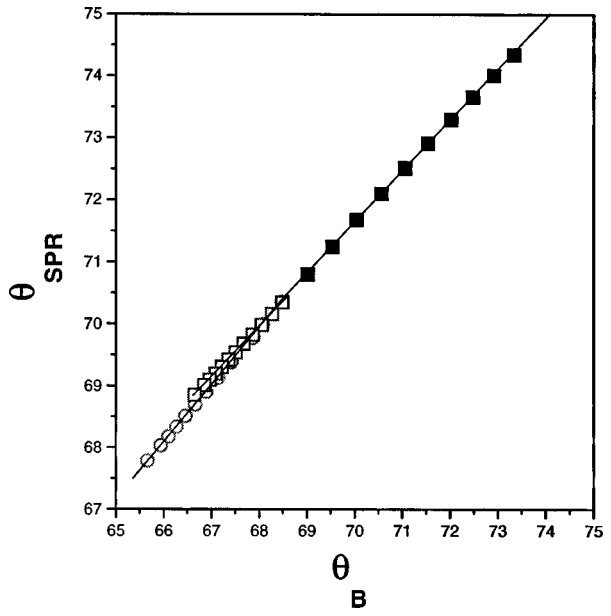

FIG. 1. Numerical modeling of the optical properties of a four-layer glass-gold-nematic-isotropic 8CB system. The liquid crystal refractive indices were taken to be $n_{\parallel}=1.6295$ and $n_{\perp}=1.5281$, from Ref. [33]. Solid squares denote the growth of a homeotropically aligned film at the substrate-isotropic interface, while the open symbols represent planar adsorbed films, with directors parallel (circles) and perpendicular (squares) to the beam direction, respectively. The angle of incidence lies above the critical angle, so that the sample is probed by an evanescent wave only. In this regime, there is a close linear relation between the Brewster angle θ_B (in degrees) and the SPR minimum in the *p*-polarized reflectivity θ_{SPR} (in degrees). Each in turn varies linearly with the film thickness, for thin enough films. In particular, with regard to Figs. 3–5 below, the linear region for homeotropic growth extends out to films of thickness 500 Å , with a shift of one degree in the Brewster angle corresponding to a change in thickness of 104 Å (3.25 times the length of an 8CB dimer [26], or about 4.5 homeotropic molecular layers). This calculation assumes a film of perfect alignment, so the thickness is really a lower bound.

modeling of the optical properties of our systems shows that this quantity is a direct measure of the thickness of an adsorbed dielectric film (Fig. 1, caption). In our study, a crucial role is played by a 20-nm film of gold to which the monolayers are bonded. That is, this thin layer of gold has a strong influence on the optical properties of our systems and, in particular, ensures that the Brewster angle θ_B lies beyond the critical angle. This makes θ_B in our experiments a sensitive probe of substrate-liquid interfaces, directly analogous to surface plasmon resonance (SPR) [9,18]. In fact, our numerical modeling of the optical properties of layered metal-dielectric systems, shows that the Brewster angle varies linearly with the position of the SPR minimum (Fig. 1). The latter is well known to vary linearly with adsorption for adsorbed films of thickness much less than the wavelength of light [19]. Quite generally, the linear Brewster angle shift is readily traced to the presence of the metallic layer [20]; otherwise the leading order behavior would be quadratic [21].

II. EXPERIMENT

The experimental arrangement of the birefringence modulated ellipsometer (Beaglehole Instruments Ltd. NZ) and temperature controlled sample cell, allows light ($\lambda = 633$ nm) incident through a prism to suffer a total internal reflection at its lower surface, at which the gold SAM layers are formed, generating an evanescent wave to interact with the liquid below. The external angle resolution is 0.03°, implying a sensitivity of better than 10^{-4} for measurements of the real and imaginary parts of the ellipticity [22]. Temperature is controlled to an accuracy of 0.01 K using a Peltier heater. Further details and diagrams are given in Ref. [9].

To generate the data presented here, two types of planar sample cells have been used. Both made use of a 60° TIH53 glass prism ($n=1.85$) onto which gold films (purity 99.99%, thickness around 20 nm) were evaporated, using an Edward 306 turbomolecular pumped coating unit at a base pressure of $\sim 2\times 10^{-6}$ mbar. Monolayers were formed by placing the gold coated prism directly into the relevant alkylthiol solution ($\sim 10^{-3}M$ in dichloromethane) for around 8 h. The surfaces were subsequently rinsed with solvent and dried in a stream of filtered nitrogen. The liquid crystal samples (obtained from Merck Ltd.) were placed between the prism SAM substrate and a lower boundary wall, that were separated by two linear spacers but left open to air in the remaining direction. Our earlier work [9] used a nonsymmetric sample cell where the far boundary was an untreated glass slide and the spacers were 125-μm optical fibers. Recent measurements were done using symmetric sample cells, where each far boundary was constructed by forming a thin gold film (thickness ~ 15 nm with 2 nm of Cr for adhesion) on a separate glass slide which was then immersed in the same SAM solution as the prism. In these cells, polytetrafluoroethylene spacers of thickness 50 μm were used to separate the two SAM surfaces. This reduction in sample cell thickness was made to lower our consumption of liquid crystal material. These cells remain much thicker than the penetration depth of the evanescent field, but one cannot rule out director-fluctuation-mediated interactions between the two opposing walls of these cells. For this reason we felt it prudent to use a far boundary with known properties. Comparison of data collected in the two types of cells, for identical monolayers and liquids, enables us to judge the significance of finite size effects. The area of the probe beam ($\sim 1\mathrm{mm}^2$) was much smaller than the surface area of the cell, so that each sample could be considered to be part of an infinite planar pore, unaffected by distant edge effects.

Measurements were taken at a series of discrete temperatures, usually starting from approximately one degree above T_{IN} and cooling the cell through the bulk isotropic to nematic phase transition of the liquid crystal to at least $0.5\,^{\circ}\mathrm{C}$ below the transition. Each temperature was monitored continuously until it stabilized, typically for 6 min, at which point a reading was recorded. The samples were then heated, to record measurements in the opposite direction, as a check on hysteresis and reproducibility of the data.

III. RESULTS

Figures 2–4 present the data in the form of a series of slices at fixed surface field h_1, for the temperature dependence of the order parameter for a set of liquid crystals of different molecular lengths *n*. The functionalized groups of the SAM surfaces COOH, OH, CH_3, and CF_3, respectively,

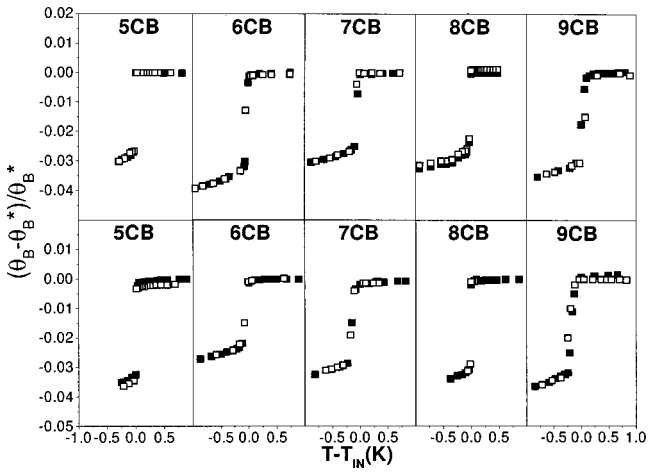

FIG. 2. Orientational wetting and anchoring data for nCB liquids on COOH (top set) and OH monolayers (bottom set). For temperatures above the isotropic-nematic bulk transition temperature (T_{IN}), the ordinate is a direct measure of the amount of nematic film adsorbed at the substrate-isotropic interface (see the caption of Fig. 1). Below T_{IN} the ordinate measures the strength of alignment in the mesoscopic region of the nematic phase probed by the evanescent field. The reduction in the Brewster angle indicates planar anchoring. Both heating (open squares) and cooling (solid squares) runs are shown.

are presented in order of increasing hydrophobicity, or decreasing surface free energies. For a quantitative measure of the associated surface field, in Table I we list the values of h_1 defined as the cosine of the receding contact angle measured for water drops placed on the SAM substrates. The reported values of θ_B have all been corrected so that they are true values, internal to the prism. We have not attempted to convert the Brewster angle measurements quantitatively into specific values of the film thickness and surface alignment, apart from approximately normalizing with respect to zero adsorption by setting the order parameter to zero at the highest temperature measured (i.e., θ_B^* is the Brewster angle measured for substrate-isotropic interfaces). Instead, we rely on the model calculations discussed with regard to Fig. 1, to achieve the following qualitative interpretation: (i) at $T > T_{IN}$, the Brewster angle changes almost linearly with the thickness of any adsorbed nematic film; and (ii) at $T < T_{IN}$, changes in the Brewster angle correspond to a temperature dependence of the nematic order parameter within a mesoscopic region near the surface (variation of the anchoring energy as temperature approaches the bulk isotropic-nematic phase transition from below).

Let us now interpret the data plotted in Figs. 2–4. First, consider the COOH-terminated monolayers. For all the nCB liquid crystals ($n=5-9$), the Brewster angle drops suddenly as temperature falls below T_{IN}. Modeling of the ellipsometric signal shows that this decrease is associated with planar (or near planar) anchoring of the nematic phase (Fig. 1). Above T_{IN} there is very little if any variation in θ_B, implying little or no temperature dependence to the interfacial structure; i.e., partial wetting or nonwetting by nematic at the substrate-isotropic interface. The data are highly reproducible between cooling and heating, except for a small temperature interval around T_{IN}. In fact, in Figs. 2 and 3 the 5CB and 8CB measurements shown are those obtained using the nonsymmetric sample cell, which in contrast to the other cases ($n=6$, 7, and 9) never showed any fluctuations at T_{IN} (except when close to an anchoring transition). This suggests that the smaller cell thickness coupled with the symmetric boundary conditions, of the latter systems, is inducing a slight hysteresis at the isotropic-nematic phase transition. If so, this could be interpreted as orientational capillary condensation. Figure 2 also shows data from another high-energy surface. An almost identical behavior is seen (the apparent decreased planar anchoring strength for 6CB may well have arisen from variations in the quality of the SAM substrates), attesting to the generic nature of the phenomena. Here a note of caution is perhaps warranted, since it is known that, in practice, OH-terminated SAM's contain a monolayer of H-bonded water molecules [12].

The hydrophobic surfaces, Figs. 3 and 4, show a much

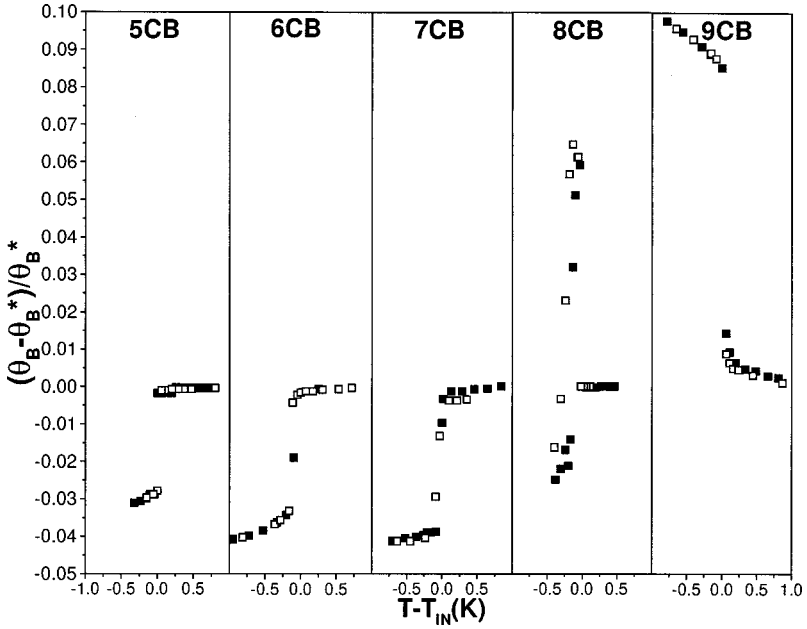

FIG. 3. Orientational wetting and anchoring data for nCB liquids on CH_3 monolayers. For temperatures above the isotropic-nematic bulk transition temperature (T_{IN}), the ordinate is a direct measure of the amount of nematic film adsorbed at the substrate-isotropic interface (see the caption of Fig. 1); note the growth of the 9CB nematic film. Below T_{IN} the ordinate measures the strength of alignment in the mesoscopic region of the nematic phase probed by the evanescent field. The reduction in the Brewster angle for the 5CB–7CB systems indicates planar anchoring while, in contrast, 9CB is homeotropically anchored. The case of 8CB adsorbed on a CH_3 monolayer lies close to an anchoring transition, between planar and homeotropic. Both heating (open squares) and cooling (solid squares) runs are shown.

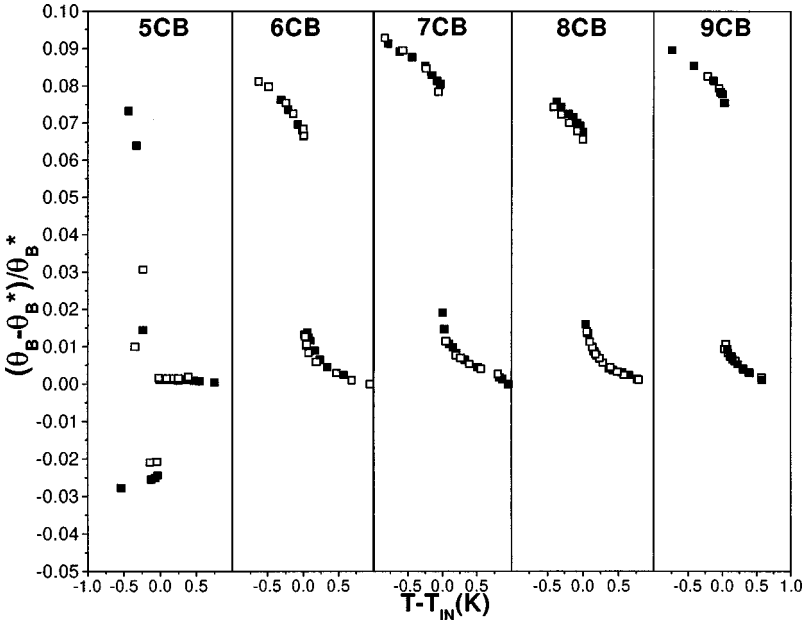

FIG. 4. Orientational wetting and anchoring data for *n*CB liquids on CF_3 monolayers. For temperatures above the isotropic-nematic bulk transition temperature (T_{IN}), the ordinate is a direct measure of the amount of nematic film adsorbed at the substrate-isotropic interface (see the caption of Fig. 1); note the continuous growth of the nematic films, for $n>5$. Below T_{IN} the ordinate measures the strength of alignment in the mesoscopic region of the nematic phase probed by the evanescent field. The increase in the Brewster angle for the 6CB–9CB systems indicates homeotropic anchoring. The case of 5CB adsorbed on a CF_3 monolayer lies close to an anchoring transition, between planar and homeotropic. Both heating (open squares) and cooling (solid squares) runs are shown.

more interesting behavior. That is, we observe two distinct classes of interfacial phase transitions. The most dramatic change in the behavior of our mesoscopic surface-alignment order parameter occurs close to 8CB on CH_3 and 5CB on CF_3, where our systems approach an anchoring transition surface in (T,n,h_1) space. This transition is highly visible in our experiments because the change in the Brewster angle on anchoring the nematic director is of opposite sign for homeotropic anchoring than that seen for planar anchoring. This behavior is readily understood from optical modeling, which also confirms the relative magnitudes involved (Fig. 1). Our data show that homeotropic anchoring of the nematic director is associated with hydrophobic surfaces, and is favored by increasing the value of *n*. The second class of phase transition is seen at $T>T_{IN}$ for those systems whose nematic director is homeotropically anchored. In particular, for 6CB–9CB on a CF_3 surface, note the continuous rise in the amount of adsorbed homeotropically aligned film as T approaches T_{IN} from above. This behavior is a class of interfacial critical phenomena, known as an approach to complete wetting [23]. In our case, since the strongly varying order parameter is molecular alignment, rather than local density, this is usually termed orientational wetting. Once again, Figs. 3 and 4 attest to the reproducibility between heating and cooling. Below, a further analysis of the orientational wetting phenomena is restricted to heating runs.

IV. DISCUSSION

The precise details of the microscopic orientational ordering within an inhomogeneous liquid crystal film cannot yet be established with current experimental techniques. This is particularly true for studies that aim to map out entire interfacial phase diagrams, as in our work. The most desired classes of order parameters are those that can clearly distinguish an adsorbed film of specific orientation from bulk isotropic phase, and yield a well-defined film thickness. Techniques such as ellipsometery and neutron reflectivity measure an integrated signal from the entire interfacial region, thereby requiring some model with which to interpret the data. The usual choice is to assume a step-function density profile, or series of step functions. For oriented films there is the additional complication that one must also model the degree of orientation. In our experiments we can clearly distinguish between planar and homeotropic order, but tilted and biaxial order, if present, would be difficult to identify in competition with variations in film thickness or anchoring strength [24]. Previous authors have taken the view that mapping their systems to coarse-grained Landau theories is one route to measuring the interfacial structure [6–8]. However, this shifts the difficulties onto interpreting the surface order parameter of a Landau theory in terms of the surface order in experiment. The former takes no account of interfacial structure arising from short-range molecular interactions (layering), and so once again is actually a measure of integrated mesoscopic order rather than microscopic surface order. The interpretation of our experiments that we suggest below is therefore subject to future verification of the precise microscopic orientational order at the SAM fluid interfaces. Note also that variation in the class of SAM surface, such as mixed monolayers of widely different chain length, liquidlike monolayers, or a different choice of thermotropic liquid crystal, will not usually be fully consistent with our systems [25]. We can however, point to the fact that our assumption of a straightforward competition between planar and homeotropic alignment is identical to the conclusion arrived at from surface forces apparatus experiments, [26], on systems of quite similar nature to ours. There is also an interesting comparison between our data and the experiments of Crawford *et al.* [27].

The data presented in Figs. 2–4 are just sufficient to en-

TABLE I. Surface field calibration.

Monolayer	$h_1 \equiv \cos\Theta$ (H_2O receding)
COOH	0.96
OH	0.87
CH_3	−0.22
CF_3	−0.39

able a sensible conjecture for the generic phase diagram depicting the orientational alignment of nCB molecules on crystalline gold-thiol SAM substrates. First, let us focus on the orientational wetting phenomena seen on low-energy surfaces. One question that arises is whether or not the underlying wetting transition is controlling the position of the anchoring transition. To grasp the nature of the thermodynamics involved, it is necessary to note the following points: (i) Orientational wetting is a class of wetting phenomena since it can be viewed as the adsorption of an A-rich film from a two-component (A-B) liquid mixture, where A is the oriented phase. (ii) Reducing T toward T_{IN} is a similar experiment to varying the chemical potential of component A at fixed T, toward bulk two-phase coexistence of A- and B-rich fluids (i.e., nematic and isotropic), which in turn is essentially equivalent to an adsorption isotherm experiment in the approach to saturation. (iii) The underlying wetting transition occurs at bulk two-phase coexistence ($T = T_{IN}$), and could be first order or continuous. (iv) An approach to complete wetting from off bulk two-phase coexistence (our experimental path) is necessarily ultimately continuous, but may involve layering and/or finite jumps in film thickness (prewetting) if the wetting transition itself is first order. (v) The equation of state of a complete wetting adsorption curve is determined by the nature of the medium- and long-range intermolecular interactions; that is, at film thicknesses in the range 2–20 molecules thick, the fluid-mediated interactions controlling the separation of the two interfaces (solid-liquid and liquid-liquid) are typically dominated by short-ranged intermolecular interactions, which in turn yield a logarithmic variation of the adsorption (the film thickness varies logarithmically with the deviation of the thermodynamic field from bulk two-phase coexistence), while for thicker films power-law dispersion interactions eventually dominate, so that the ultimate divergence of the adsorption will be power law.

In our experimental setup it is difficult to collect meaningful adsorption data at film thicknesses beyond ten molecular lengths, since to grow thicker equilibrium films would require very fine control over the thermodynamic field T, and the evanescent field decay would need to be taken into account. So the physics of wetting summarized above suggests the appropriate treatment of our complete wetting data is to plot thickness (i.e., Brewster angle) vs the logarithm of $(T-T_{IN})/T_{IN}$. Such a plot should be linear with a slope whose magnitude defines the exponential decay length of the fluid mediated interactions (arising from short-range intermolecular forces) between the two interfaces on either side of the adsorbed film (note that an approach to complete wetting can equally well be regarded as interface delocalization), [28]. Figure 5 displays all our wetting data on nematic films of nCB on low-energy surfaces, in this form. Each plot is linear within experimental error (which we note grows uncontrollably large in the limit of extremely small $T-T_{IN}$), showing consistency with complete wetting. However, this does not rule out the possibility of pseudo wetting (contact angle just above zero) if the asymptotic power-law interactions were to be unfavorable. Optical modeling (Fig. 1, caption) shows that the plots in Fig. 5 cover a range of thicknesses equivalent to a little over three perfectly oriented dimer layers (4–5 molecular lengths), so our complete wetting data imply that the exponentially decaying interaction between the substrate-nematic interface and the nematic-isotropic interface has a decay length (or correlation range) of about the length of one nCB dimer.

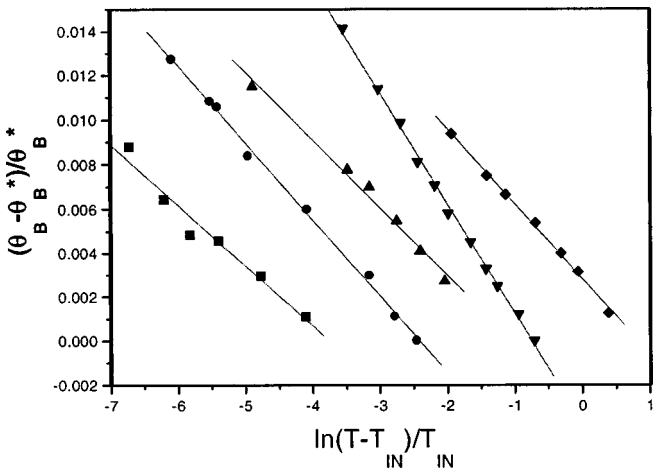

FIG. 5. Heating data from Figs. 3 and 4, replotted to highlight that the observed growth of nematic films at interfaces between low-energy monolayers and isotropic nCB liquids is consistent with complete wetting by nematic at $T=T_{IN}$. The abscissa scale shown applies only to the case of 9CB adsorbed on a CH_3 monolayer (solid squares), with the remaining plots (from left to right: 6CB–9CB on CF_3) shifted horizontally, for clarity.

Turning now to the data at $T<T_{IN}$, we note that our 8CB on CH_3 and 5CB on CF_3 systems clearly lie close to an anchoring transition surface in (T,n,h_1) space. That is, we interpret this wildly but slowly fluctuating data as arising from director fluctuations (domains of planar and homeotropically anchored nematic wandering in and out of the beam spot). Note also that the complete wetting signature has now disappeared at $T>T_{IN}$. It is therefore tempting to conclude that in our systems the presence of complete orientational wetting is present whenever the anchoring is homeotropic, so that the anchoring transition surface intersects the plane of bulk two-phase coexistence precisely at the curve of wetting transitions. Figure 6 shows the qualitative orientational wetting and anchoring phase diagram that follows from this interpretation. It is of course automatic that complete orientational wetting by, say, homeotropic demands homeotropic anchoring at $T=T_{IN}$, but it is not obvious that the reverse implication need hold. To test this issue further would require us to home in on the wetting transition curve. For example, one could use mixtures of 5CB and 6CB on a CF_3 substrate, and vary the concentration. If the complete wetting signature disappeared suddenly then the wetting transition at $T=T_{IN}$ is first order. Alternatively, two-component SAM's composed of a mixture of CH_3 and CF_3 thiols could be used to approach the wetting transition near, say, 8CB on a CH_3 substrate. In fact, a successful preliminary demonstration of this latter experiment is given in Fig. 6 of Ref. [9].

Let us now address the somewhat counterintuitive result that our low-energy surfaces (CH_3,CF_3) induce complete wetting by a nematic film, whereas the high-energy surfaces (COOH, OH) are partially wet or nonwet. The appearance of a thick wetting film at an interface reflects the outcome of a balance of three interfacial free energies. This need not de-

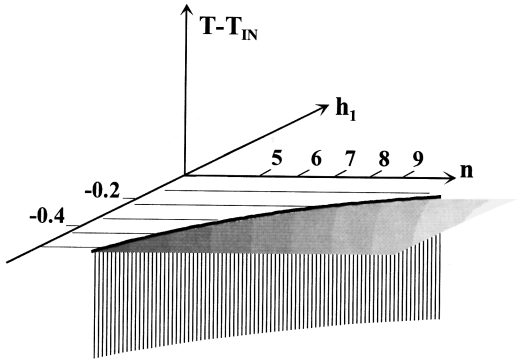

FIG. 6. A schematic phase diagram depicting all of the anchoring and orientational wetting phenomena observed in Figs. 2–5. The h_1 axis is labeled by values listed in Table I. The vertical striped sheet denotes an anchoring transition surface, between planar (low n) and homeotropic (high n) surfaces. This sheet meets the bulk two-phase coexistence surface, the (n,h_1) plane, in a line of orientational wetting transitions. In this plane the densely shaded region denotes complete wetting by homeotropic films. The lightly shaded region denotes partial wetting or nonwetting by nematic films.

mand high-energy substrates; e.g., from statistical mechanical models we know that vapor completely wets the interface between saturated liquid and a hard wall (liquid-liquid attractions favor liquid to be separated from the zero-energy wall) [29,30]. In the case of nCB liquids, the molecules are known to favor dimer formation, with the alkyl tails pointing roughly in opposite directions (see Ref. [26] and references therein), due to head-head attraction. This in turn favors the formation of smectic clusters, with larger values of n (blunter ends to the dimers) associated with an enhanced tendency to smectic order (provided n is not so large that liquid crystalline behavior is destabilized) [31]. It is probable that this quasismectic order is enhanced in the region adjacent to our substrates, since a planar wall is a strong smectic field. The proposed interpretation of our data is that a sufficiently low-energy surface yields homeotropic anchoring because of a preference arising from nCB-nCB interactions and/or entropy, which in turn favors complete wetting by nematic. Planar alignment is driven by wall-liquid energy, which is apparently sufficiently disruptive of nCB-nCB correlations to prevent orientational wetting by planar nematic films.

Finally, we emphasize that our phase diagram is specific to the thiol-SAM–nCB systems under study. It is not true that every high-energy surface will induce planar alignment, and in fact we have found that bare gold (no SAM layer) anchors 8CB molecules homeotropically. This presumably reflects the fact that the presence of a SAM of sufficient thickness effectively screens the adsorbed fluid from the underlying gold, while bare gold possesses strong medium-range dispersion interactions with adsorbed nCB molecules [32].

ACKNOWLEDGMENTS

This work was supported by the Engineering and Physical Sciences Research Council. We also wish to acknowledge Professor A. Ulman for providing the perfluorinated thiol material and Dr. D. Coates (Merck Ltd., U.K.) for a kind gift of liquid crystals.

[1] S. Chandrasekhar, *Liquid Crystals* (Cambridge University Press, Cambridge, 1977).
[2] B. Jerome, Rep. Prog. Phys. **54**, 391 (1991).
[3] T. J. Sluckin and A. Poniewierski, in *Fluid Interfacial Phenomena*, edited by C. A. Croxton (Wiley, New York, 1986).
[4] B. Jerome, J. Phys.: Condens. Matter **6**, A269 (1994); Mol. Cryst. Liq. Cryst. **251**, 219 (1994).
[5] S. Faetti, M. Gatti, V. Palleschi, and T. J. Sluckin, Phys. Rev. Lett. **55**, 1681 (1985).
[6] K. Miyano, J. Chem. Phys. **71**, 4108 (1979).
[7] H. Hsiung, Th. Rasing, and Y. R. Shen, Phys. Rev. Lett. **57**, 3065 (1986).
[8] W. Chen, L. J. Martinez-Miranda, H. Hsiung, and Y. R. Shen, Phys. Rev. Lett. **62**, 1860 (1989).
[9] S. D. Evans, H. Allinson, N. Boden, and J. R. Henderson, Faraday Discuss. **104**, 37 (1996).
[10] R. A. Drawhorn and N. L. Abbott, J. Phys. Chem. **99**, 16 511 (1995).
[11] A. Ulman, *An Introduction to Ultrathin Organic Films: From Langmuir-Blodgett to Self-Assembly* (Academic, New York, 1991).
[12] A. Ulman, S. D. Evans, Y. Shnidman, R. Sharma, J. E. Eilers, and J. C. Chang, J. Am. Chem. Soc. **113**, 1499 (1991).
[13] C. D. Bain, J. Evall, and G. M. Whitesides, J. Am. Chem. Soc. **111**, 7155 (1989).
[14] We have confirmed that this perfluorinated material produces well-defined quasicrystalline surfaces. Atomic force microscope images of the SAM surface show that the molecules pack on a hexagonal lattice, with a lattice constant of 5.3 Å .
[15] F. Heslot, A. M. Cazabat, and N. Fraysse, J. Phys.: Condens. Matter **1**, 5793 (1989).
[16] R. M. A. Azzam and N. M. Bashara, *Ellipsometry and Polarised Light* (North-Holland, Amsterdam, 1989).
[17] D. Beaglehole, Physica B & C **100**, 163 (1980); J. Lekner, *Theory of Reflection* (Nijhoff/Kluwer, Dordrecht, 1987).
[18] S. D. Evans, H. Allinson, N. Boden, T. M. Flynn, and J. R. Henderson, J. Phys. Chem. B **101**, 2143 (1997).
[19] G. W. Bradberry, P. S. Vukusic, and J. R. Sambles, J. Chem. Phys. **98**, 651 (1993).
[20] D. Beaglehole (private communication).
[21] J. Lekner, Pure Appl. Opt. **3**, 821 (1994).
[22] S. N. Jaspeson and S. E. Schnatterly, Rev. Sci. Instrum. **40**, 761 (1969).
[23] See, for example, D. E. Sullivan and M. M. Telo da Gama, in *Fluid Interfacial Phenomena*, edited by C. A. Croxton (Wiley, New York, 1986).
[24] Notwithstanding these difficulties, we are able to rotate the sample prism, thereby exposing different faces to the ellipsometer beam. For 5CB on a CH_3 surface, this experiment yielded a clear shift in the planar anchoring Brewster angle (at $T < T_{IN}$), suggesting the presence of biaxial planar alignment.
[25] V. K. Gupta, W. J. Miller, C. L. Pike, and N. L. Abbott, Chem.

Mater. **8**, 1366 (1996); V. K. Gupta and N. L. Abbott, Langmuir **12**, 2587 (1996).
[26] M. Ruths, S. Steinberg, and J. N. Israelachvili, Langmuir **12**, 6637 (1996).
[27] G. P. Crawford, R. J. Ondris-Crawford, J. W. Doane, and S. Zumer, Phys. Rev. E **53**, 3647 (1996).
[28] E. Brezin, B. I. Halperin, and S. Leibler, Phys. Rev. Lett. **50**, 1387 (1983); J. R. Henderson, Mol. Phys. **62**, 829 (1987); Phys. Rev. E **50**, 4836 (1994).
[29] J. R. Henderson and F. van Swol, Mol. Phys. **56**, 1313 (1985).
[30] An even closer analogy is the complete wetting of the free surface of 5CB, by homeotropic nematic [J. V. Selinger and D. R. Nelson, Phys. Rev. A **37**, 1736 (1988)].
[31] F. Affouard, M. Kroger, and S. Hess, Phys. Rev. E **54**, 5178 (1996).
[32] W. J. Miller and N. L. Abbott, Langmuir **13**, 7106 (1997).
[33] S. J. Elston and J. R. Sambles, *The Optics of Thermotropic Liquid Crystals* (Taylor & Francis, London, 1992).